

Swellable, Water- and Acid-Tolerant Polymer Sponges for Chemoselective Carbon Dioxide Capture

Robert T. Woodward,[†] Lee A. Stevens,[‡] Robert Dawson,[†] Meera Vijayaraghavan,[†] Tom Hasell,[†] Ian P. Silverwood,[§] Andrew V. Ewing,[§] Thanchanok Ratvijitvech,[†] Jason D. Exley,^{||} Samantha Y. Chong,[†] Frédéric Blanc,[⊥] Dave J. Adams,[†] Sergei G. Kazarian,[§] Colin E. Snape,[‡] Trevor C. Drage,[‡] and Andrew I. Cooper^{*,†}

[†]Department of Chemistry and Centre for Materials Discovery and [⊥]Department of Chemistry and Stephenson Institute for Renewable Energy, University of Liverpool, Crown Street, Liverpool, L69 7ZD, United Kingdom

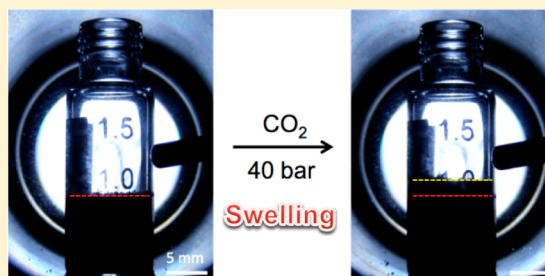
[‡]Department of Chemical and Environmental Engineering, Faculty of Engineering, University of Nottingham, University Park, Nottingham, NG7 2RD, United Kingdom

[§]Department of Chemical Engineering, Imperial College London, South Kensington Campus, London, SW7 2AZ, United Kingdom

^{||}Micromeritics Instrument Corporation, 4356 Communications Drive, Norcross, Georgia 30093, United States

Supporting Information

ABSTRACT: To impact carbon emissions, new materials for carbon capture must be inexpensive, robust, and able to adsorb CO₂ specifically from a mixture of other gases. In particular, materials must be tolerant to the water vapor and to the acidic impurities that are present in gas streams produced by using fossil fuels to generate electricity. We show that a porous organic polymer has excellent CO₂ capacity and high CO₂ selectivity under conditions relevant to precombustion CO₂ capture. Unlike polar adsorbents, such as zeolite 13x and the metal–organic framework, HKUST-1, the CO₂ adsorption capacity for the hydrophobic polymer is hardly affected by the adsorption of water vapor. The polymer is even stable to boiling in concentrated acid for extended periods, a property that is matched by few microporous adsorbents. The polymer adsorbs CO₂ in a different way from rigid materials by physical swelling, much as a sponge adsorbs water. This gives rise to a higher CO₂ capacities and much better CO₂ selectivity than for other water-tolerant, nonswellable frameworks, such as activated carbon and ZIF-8. The polymer has superior function as a selective gas adsorbent, even though its constituent monomers are very simple organic feedstocks, as would be required for materials preparation on the large industrial scales required for carbon capture.



INTRODUCTION

The use of fossil fuels to generate electricity is the single largest anthropogenic source of CO₂ emissions. Carbon capture and storage (CCS) represent a rapidly developing set of technologies that includes precombustion capture, postcombustion capture, and oxyfuel combustion capture. CCS has the potential to achieve >90% reductions in CO₂ emissions.¹ All variants of CCS involve gas separation on multiton scales to achieve a highly concentrated stream of CO₂ for transport and subsequent storage. However, significant cost reductions are required to render CCS technologies competitive with other low-carbon generation technologies, such as renewables and nuclear power. A key target is to lower the dominant energy penalty, and therefore the cost, associated with the CO₂ separation process.

In precombustion CO₂ capture, an integrated gasification combined cycle (IGCC) power station uses the water–gas shift reaction to convert gasified fuel into a mixture of hydrogen and CO₂. The CO₂ must then be separated before using the hydrogen to drive a combined cycle turbine for electricity

generation.² Hence, the challenge is to separate CO₂ and hydrogen (H₂) on a large scale in an energy efficient way, while minimizing hydrogen losses. The current state-of-the-art technology for precombustion capture uses physical solvent systems, such as the Selexol technology in a pressure-swing cycle.³ Other, next-generation technologies for precombustion CO₂ separation include membranes with selective permeability^{4,5} and porous adsorbents.^{6,7}

There are stringent technical and economic requirements for solid adsorbents for precombustion CO₂ capture. The adsorbent must operate in a gas stream leaving the water–gas shift reactor at a total pressure of approximately 30–45 bar and at a temperature of around 40 °C. The CO₂ mole fraction would be approximately 35–40%, and hence the partial pressure of CO₂ would be approximately 12–18 bar. The major component is the gas-shifted fuel, H₂ (>60 mol %). The pressure and temperature of the gas stream make pressure-

Received: March 31, 2014

Published: May 29, 2014

swing cycles particularly attractive.⁸ An adsorbent must have a large CO₂ sorption capacity if it is to form part of an economically viable separation process. It must also have good selectivity for the adsorption of CO₂ with respect to other components in the gas stream in order to generate a CO₂ stream of the required purity. In particular, it must adsorb CO₂ in preference to the major component, H₂, and also other minor components such as water vapor and nitrogen (N₂). Selectivity is related to adsorption thermodynamics: the CO₂ must be adsorbed just strongly enough to facilitate the separation, without generating a large energy penalty in regenerating the adsorbent. More specifically, porous materials are required that can separate out a high-purity CO₂ stream at elevated pressures without the need for a vacuum regeneration cycle, which would add a significant energy penalty. A candidate adsorbent must also have good physicochemical stability: it must be moisture stable, thermally stable, and insensitive to corrosive acidic gases such as hydrogen sulfide over long periods. Finally, given the enormous volumes of CO₂ to be captured, candidate materials for CCS must be relatively inexpensive and their preparation must be scalable. For example, the proposed Don Valley, UK, 920 MW IGCC plant could potentially produce up to 14,000 tons of CO₂ per day in routine operation. Hence, while there have been major advances in the chemical synthesis of new porous solids with atomic precision,^{9,10} most materials will fail for precombustion CCS on at least one of the five primary criteria of CO₂ capacity, CO₂ selectivity, sorption energetics, physicochemical stability, and cost.

Porous metal–organic frameworks (MOFs) have been studied intensively as adsorbents for CCS.^{11–13} Exceptional surface areas of up to 7000 m²/g are possible in MOFs,¹⁴ and ultralow-density frameworks, such as MOF-210, can show extraordinary CO₂ uptakes (54.5 mmol/g at 50 bar CO₂ pressure and 298 K).¹⁵ Synthetic strategies have also been devised to optimize CO₂ selectivity, for example by using mixed organic linkers in “multivariate” MOFs.¹⁶ However, the practical potential of most “ultraporous” MOFs, such as MOF-210, is curtailed by limited physicochemical stability and, particularly, by sensitivity to water. More stable MOFs with lower surface areas, such as zinc imidazolate frameworks (ZIFs),¹⁷ might be better candidates for practical CCS. However, even ZIF-8, one of the more stable MOFs, has been shown undergo hydrolysis unless suitably protected.¹⁸

Microporous organic polymers can combine high levels of porosity with good chemical stability.¹⁹ For example, a polyphenylene network, PAF-1, has a surface area of 5,600 m²/g and an excess CO₂ uptake of 29.5 mmol/g at 40 bar CO₂ pressure and 298 K.²⁰ The physicochemical stability of PAF-1 is excellent: boiling in water for 7 days has no effect on its gas sorption properties. However, scale up may be challenging because the tetraphenylmethane-derived monomer for PAF-1 is quite expensive. More seriously, PAF-1 must be synthesized under rigorously anhydrous and anaerobic conditions, typically in a glovebox, because the stoichiometric nickel coupling reagent is air and moisture sensitive.²⁰ Indeed, the economics of scale-up is a general concern for porous polymer adsorbents that are prepared using precious metal reagents or catalysts, such as most conjugated microporous polymers.²¹

Extremely high surface areas may not, in fact, be a prerequisite for CCS, particularly if the sorption affinity of the adsorbent is thermodynamically attuned for CO₂ adsorption. Several studies have focused on microporous

polymers with chemical functionality that was selected to improve gas selectivity, mainly in the context of postcombustion CCS where the pressure is 1 bar.^{22,23} The introduction of polar functional groups into polymers can greatly improve selectivity for CO₂ over nitrogen (N₂)^{23–25} by introducing specific intermolecular interactions with the CO₂ molecules.²⁶ However, it has also been shown that polar groups can enhance water uptake, too, thus leading to an overall decrease in CO₂ sorption capacity when measurements are performed under more realistic conditions in the presence of water vapor.²⁷ As such, increasing the polarity of porous polymers, while effective under laboratory conditions for perfectly dry CO₂ gas streams, will not necessarily translate into practical benefits for real-life CCS.

Hyper-cross-linked polymers^{28,29} are scalable porous materials that have been produced commercially for some years. Recently, hyper-cross-linked polymers were synthesized using a formaldehyde dimethyl ether cross-linker,³⁰ extending the approach to a wide range of low functionality aromatic monomers. Indeed, the monomer can be as simple and inexpensive as benzene (Figure 1), and the materials cost is

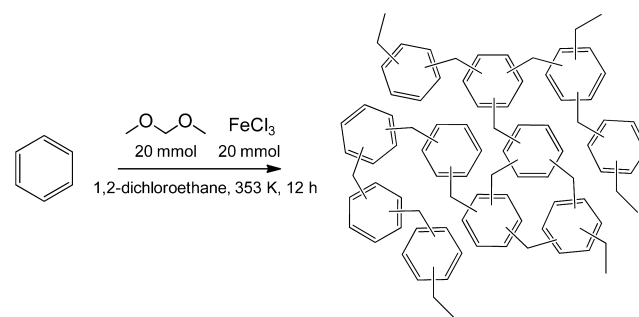


Figure 1. Synthesis of porous polymer network, **1**. Friedel–Crafts alkylation of benzene with 2 equiv of formaldehyde dimethyl acetal produces a microporous, “knitted” hyper-cross-linked polymer network.

therefore determined by the dimethyl ether cross-linker, which is used stoichiometrically, and the solvent, although it is possible that the latter could be either recycled or avoided completely: for example, by carrying out reactions in the neat aromatic monomer. Hyper-cross-linked polymers have moderate CO₂ uptakes at low pressures (1 bar), but they show more promising CO₂ uptakes at the higher pressures that are relevant to precombustion CCS.³¹

Unlike porous crystals such as MOFs and zeolites, hyper-cross-linked polymers exist in a state that is far from thermodynamic equilibrium. As synthesized, they form expanded, solvent-swollen networks. These networks then collapse upon removal of the solvent, but cannot collapse fully to a nonporous state because of the high cross-linking levels. This introduces considerable strain in the network.³² Consequently, these materials are predisposed to swell in a wide range of solvents, including thermodynamically “bad” solvents for the polymers.³³ Carbon dioxide is known to swell nonporous aromatic polymers, such as polystyrene,³⁴ and we speculated, therefore, that porous hyper-cross-linked polymers might adsorb CO₂ by a chemospecific swelling mechanism that is not accessible in rigid, crystalline porous frameworks.

RESULTS AND DISCUSSION

The Friedel–Crafts alkylation reaction shown in Figure 1 was carried out for four different aromatic monomers: benzene (polymer 1), tetraphenylmethane (polymer 2), triphenylmethane (polymer 3), and triptycene (polymer 4). The details of all materials are included in the Supporting Information, but only the benzene network, 1, is discussed here. Polymers 2–4 did not give any real functional advantage for CCS, and their monomers are all much more expensive than benzene. All polymers were produced as insoluble dark brown solids with yields greater than 90% on a typical laboratory preparative scale of 5–10 g per batch.

The amorphous and insoluble nature of these polymers makes their structural characterizations challenging, and this relies extensively on solid-state magic angle spinning (MAS) NMR spectroscopy. Although this approach is powerful, acquisition of the NMR spectra is time-consuming (hours or days), especially when libraries of polymers are synthesized. It was shown that the sensitivity issue in solid-state NMR could be tackled with high-field dynamic nuclear polarization (DNP)^{35–41} using a transfer of polarization from electrons (added to the samples as mono³⁵ or biradicals^{42–44}) to nuclear spins at cryogenic temperatures and under adequate DNP sample preparation condition.^{35,37} We have recently exploited this strategy for high-throughput structural NMR characterization of microporous organic polymers⁴⁵ where we showed that ¹³C cross-polarization (CP) magic angle spinning (MAS) NMR could be obtained in minutes only.

The DNP enhanced ¹³C CP MAS NMR spectra of polymer 1 obtained at a field strength of 14.1 T is given in Figure S29. This revealed the presence of substituted and nonsubstituted aromatic carbon at 137 and 130 ppm as well as the CH₂ bringing linker at 36 ppm.³⁰ A weak signal, hardly visible in the spectra without DNP, is also observed at 20 ppm and is assigned to a CH₃ group corresponding to the methylation of benzene with the acetal. The NMR spectra for network polymer 1 (with 3 equiv of cross-linker), the same polymer with 4 equiv of cross-linker, and polymer 3 were all very similar. They also showed a small CH₃ peak (in addition to the expected CH signal of the triphenylmethane moiety in the cages of 3 at 48 ppm).

The polymers were microporous, as indicated by a steep uptake at low relative pressures in nitrogen adsorption isotherms (Figure 2; see Figure S1 for isotherms for polymers 2–4).

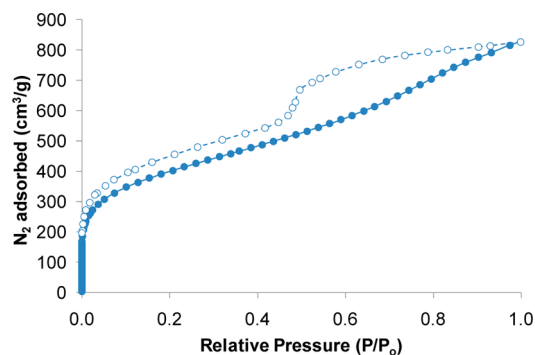


Figure 2. Nitrogen sorption isotherm for 1. Adsorption (solid symbols) and desorption (open symbols) isotherms at 77 K indicates microporosity. The hysteresis loop suggests swelling.

The hysteresis loop in the desorption isotherm is consistent with swelling of the network during sorption analysis at 77 K.⁴⁶ The apparent BET surface area (1228 m²/g), the total pore volume (1.54 cm³/g), and the micropore volume (0.46 cm³/g) were calculated from the low-pressure nitrogen isotherm. The other hyper-cross-linked polymers, 2–4, had broadly similar properties (Table S1).

To evaluate its potential for precombustion CCS, polymer 1 was compared with four other porous solids: an activated carbon (Norit R2030, Norit Carbon UK; a steam-activated carbon specifically designed for CO₂ applications), a polar zeolite, zeolite 13x,⁴⁷ and two robust metal–organic frameworks, ZIF-8¹⁷ and HKUST-1.⁴⁸ The porous properties of these materials, as derived from nitrogen sorption analyses, and their bulk densities, are given in Table 1.

Table 1. Porous Properties of the Adsorbents Tested

network	SA _{BET} ^a (m ² /g) ^a	micropore volume (cm ³ /g) ^a	bulk density (g/cm ³)
polymer 1	1228	0.46	0.35 ^b
carbon	806	0.30	0.52 ^c
zeolite 13x	848	0.31	0.35 ^c
ZIF-8	2188	0.65	0.35 ^c
HKUST-1	1896	0.73	0.48 ^c

^aCalculated from N₂ sorption isotherms measured at 77 K for “dry” samples which had been degassed at 120 °C for 15 h under high vacuum (<15 μbar). ^bMeasured using mercury intrusion porosimetry at 0.31 psi. ^cData from suppliers of materials.

Our strategy was to evaluate all of these materials in terms of four key properties that might define their performance in precombustion CCS, namely; (i) CO₂ sorption capacity; (ii) tolerance to water and acids; (iii) CO₂/H₂ selectivity; and (iv) CO₂/N₂ selectivity. The results of these measurements are summarized in Table 2.

First, the single component CO₂ isotherms were measured for all samples in the “dry”, thoroughly degassed state up to a pressure of 40 bar using high-purity CO₂. Total pressures of around 40 bar are relevant to precombustion CCS¹² (even higher-pressure systems might be developed in the future), but we also analyzed these data in terms of sorption capacities at 17.5 bar, which is more reflective of the likely partial pressure of CO₂ in precombustion CCS.

Of the five materials tested, polymer network 1 has the highest gravimetric CO₂ capacity of 15.32 mmol/g in the “dry” state at 40 bar, as compared to values in the range 6.91–9.30 mmol/g for the other four materials. It also has the highest gravimetric CO₂ capacity at the lower pressure of 17.5 bar (8.66 mmol/g). Polymer 1 does not, however, have the highest apparent BET surface area or micropore volume, as measured by N₂ adsorption: both of the MOFs, ZIF-8 and HKUST-1, have higher porosity as measured in that way (Table 1). The isosteric heat of adsorption for CO₂ was measured for 1 and was found to be 28–30 kJ/mol at low CO₂ coverage (Figure S2): this is comparable with other porous polymers and not high enough to introduce large energy penalties for CO₂ desorption.

These “dry” measurement conditions involve rigorous degassing of the sample before analysis (<15 × 10⁻⁶ bar, 120 °C, 15 h). Such high vacuum conditions would be prohibitively expensive for CCS. Also, in real CCS, the adsorbent would not be exposed to high-purity CO₂. Instead, the regenerated

Table 2. Key Functional Properties for Porous Adsorbents for Precombustion CCS^a

network	CO ₂ uptake (mmol/g) ^b		H ₂ uptake (mmol/g) ^b		N ₂ uptake (mmol/g) ^b		CO ₂ /H ₂ selectivity ^d		CO ₂ /N ₂ selectivity ^d	swelling in CO ₂ ^e (%)	volumetric CO ₂ uptake (mmol/cm ³)
	dry ^c	wet ^c	dry ^c	wet ^c	dry ^c	wet ^c	dry ^c	wet ^c	dry ^c		wet ^f
polymer 1	15.32 (8.66)	13.17 (7.12)	0.68 (0.29)	0.58 (0.30)	2.65 (1.61)	2.43 (1.42)	22.5 (29.9)	22.7 (23.7)	5.8 (5.4)	11.2 (4.3)	4.61 [3.63] ^h (2.50) [2.39] ^h
carbon	6.91 (6.33)	5.75 (3.10)	1.35 (0.61)	0.61 (0.34)	3.50 (2.39)	1.96 (1.25)	5.1 (10.4)	9.4 (9.1)	2.0 (2.6)	0 (0)	2.99 (1.61)
zeolite 13x	8.03 (7.40)	0.46 (0.19)	0.56 (0.26)	— ^g	2.89 (2.09)	— ^g	14.3 (28.5)	— ^g	2.8 (3.5)	0 (0)	0.16 (0.07)
ZIF-8	9.30 (7.74)	8.78 (6.99)	0.84 (0.32)	0.67 (0.33)	2.32 (1.31)	2.21 (1.19)	11.1 (24.2)	13.1 (21.2)	4.0 (5.9)	0 (0)	3.07 (2.45)
HKUST-1	7.91 (7.37)	2.19 (0.67)	0.96 (0.44)	— ^g	3.23 (2.18)	— ^g	8.2 (16.8)	— ^g	2.4 (3.4)	0 (0)	1.05 (0.32)

^aPolymer 1 outperforms the other materials significantly in terms of gravimetric CO₂ uptake and CO₂/H₂ selectivity (both dry and wet conditions; see also Figure 3f. ^bGravimetric CO₂ capacity as measured in pure CO₂ at 40 bar, 298 K; in all cases, figures in parentheses refer to data measured at 17.5 bar, reflecting the likely partial pressure of CO₂ in precombustion CCS. ^c“Dry” samples were degassed under dynamic vacuum at 120 °C (<15 × 10⁻⁶ bar) for 15 h before analysis; “wet” samples were equilibrated with air for 48 h and were *not* degassed before analysis. ^dIdeal molar gas selectivities as calculated from independent sorption isotherms for pure gases; the ratios were calculated at 40 bar, 298 K. ^eChange in sample volume between 1 and 40 bar, as estimated using a high-pressure view cell (±1.3%). ^fCalculated from “wet” CO₂ sorption data using the material density values given in Table 1; in real CCS, it would be the packed pellet density, rather than the bulk material density used here, that will determine the size of the CO₂ capture unit. ^gGas uptake under these conditions was too low to be quoted with precision. ^hFigures in square brackets are data corrected to allow for volume increase in the sample upon polymer swelling, reflecting the fact that sample volume determines the overall size of the capture unit required.

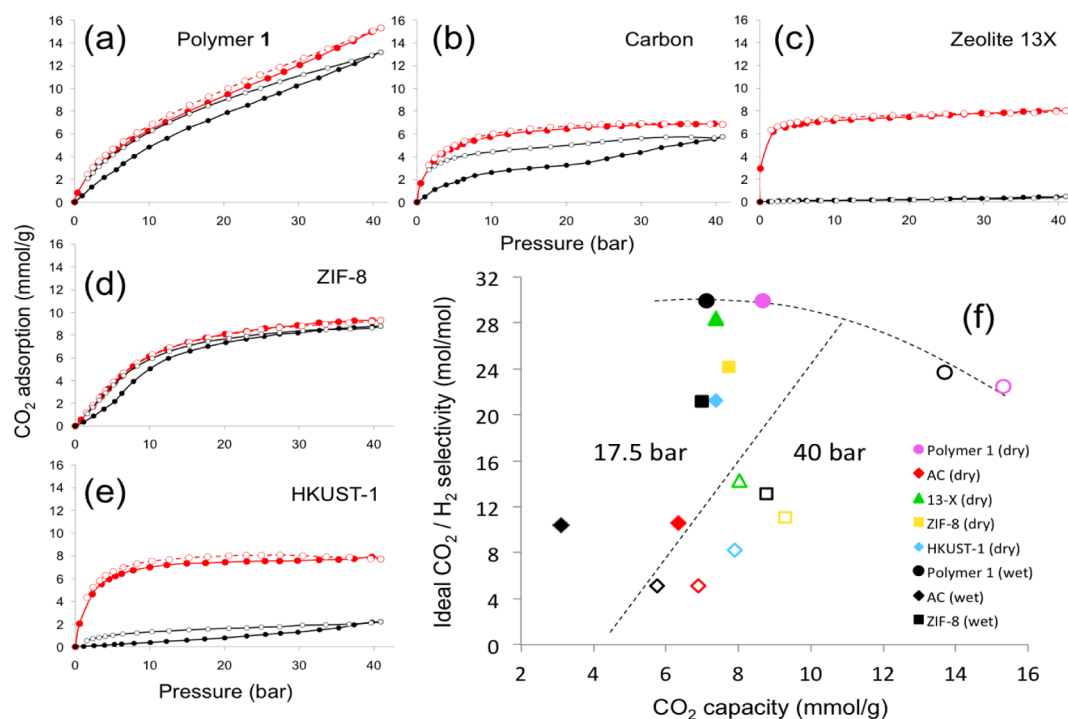


Figure 3. Gas sorption isotherms for wet and dry adsorbents (a–e) and their ideal CO₂/H₂ selectivities (f). For (a–e), the x-axis represents pressure (in bar), and the y-axis represents CO₂ adsorption in mmol/g. Adsorption (solid circles) and desorption (open circles) isotherms (100% CO₂) for both “dry” (red) and “wet” (black) samples of (a) benzene polymer 1; (b) activated carbon R2030; (c) zeolite 13x; (d) ZIF-8; and (e) HKUST-1. (f) The ideal CO₂/H₂ selectivity plotted against CO₂ capacity, as measured at 40 bar (open symbols to right of dashed straight line) and 17.5 bar (likely CO₂ partial pressure in precombustion CCS; closed symbols to left of line). Colored symbols denote “dry” measurements and black symbols denote the corresponding “wet” measurements. Wet uptakes for HKUST-1 and zeolite 13x are not plotted because both CO₂ and H₂ uptakes are very low in the presence of physisorbed water. Polymer 1 (circle points) forms the upper performance bound for the five materials, as illustrated by the curved, dotted line.

adsorbent would be exposed to a mixture of CO₂ with other components such as H₂, N₂, and water vapor. We showed previously that exposure to atmospheric water vapor can have a large, negative influence on the CO₂ capacity of otherwise promising porous polymer adsorbents for postcombustion

CCS.²⁶ Hence, the CO₂ capacities of all samples were remeasured after exposure to air for 48 h (22 °C, 35–45% relative humidity), in the absence of the high-vacuum degassing step, to more closely mimic real-life CCS conditions. In some cases, the CO₂ capacities in the “wet” samples were dramatically

lower than the corresponding dry measurements. For example, the MOF sample, HKUST-1, retained only 28% of its dry CO₂ capacity at 40 bar when wet,⁴⁹ although we note that other studies show an enhancement in CO₂ uptake in HKUST-1, at least at lower pressures, at certain levels of framework hydration.⁴⁸ Water was also shown by others to have a highly deleterious effect on CO₂ sorption for the magnesium MOF, Mg-MOF-74.⁵¹ The effect on zeolite 13x is even more striking: it has just 6% of its dry CO₂ capacity at 40 bar when wet, not because it is unstable to water but because the material is strongly hydrophilic. It is a much better adsorbent for water than for CO₂, and dehydration is energy intensive. By contrast, the three more hydrophobic materials, polymer **1**, activated carbon, and ZIF-8, retain between 83% and 94% of their dry CO₂ capacity at 40 bar when wet (86% for **1**). Similar conclusions can be drawn from CO₂ sorption data at 17.5 bar.

In addition to retaining CO₂ selectivity under moist conditions, more hydrophobic materials may also exhibit better chemical stability to water and to acidic impurities in the gas stream. To demonstrate this, samples of polymer **1** were boiled in both water and in aqueous sulfuric acid (1 M) for 1 h. This had no effect on either the porosity or the CO₂ uptake (Figures S3 and S4), indicating excellent stability, both to water and to acid. Analysis by Fourier transform infrared (FTIR) spectroscopy also showed no chemical change to the polymer after boiling in concentrated acid (Figure S5). By contrast, many porous inorganic materials or hybrid MOFs would be rendered nonporous or dissolved by boiling in acidic solutions.

Water adsorption isotherms were also measured for polymer **1** at 1 bar and 298 K, and this showed that there is very little water uptake until humidity reaches a high level (Figure S6), which is consistent with the selective adsorption of CO₂ over water in **1**. Taken together, these data suggest a strong advantage for more hydrophobic adsorbents for precombustion CCS in terms of avoiding the energy penalties associated with rigorous drying of either the adsorbent or the gas stream.

The CO₂ sorption isotherms for the various dry and wet samples are shown in Figure 3. In addition to its higher CO₂ capacity, the relative shapes of the isotherms reveal another advantage for polymer **1**. The working capacity, rather than the absolute capacity, will define the performance of an adsorbent. The working capacity is defined as the difference between the quantity of CO₂ adsorbed at the adsorption pressure, and the residual adsorbed CO₂ at the desorption pressure, in the pressure swing cycle.⁴¹ In general, the introduction of larger pressure swings in CCS introduces additional energy penalties, and hence materials that can adsorb and release large amounts of CO₂ over a small operational pressure window are desirable. The greater slope of the adsorption/desorption isotherms for **1** at higher pressures is therefore an advantage in a pressure-swing adsorption/desorption cycle. This is related to swelling effects, as discussed below.

For precombustion CO₂ capture, good CO₂:H₂ selectivity at high pressures is paramount. We therefore measured the H₂ isotherms for this set of materials over the same pressure range, 1–40 bar (Figure S7). From these data, it was possible to calculate an ideal CO₂:H₂ selectivity, defined simply as the ratio of the CO₂ and H₂ uptakes at a given pressure. This is shown for all five materials at two pressures, 17.5 and 40 bar, in Figure 3f. The “wet” H₂ sorption capacities reflected the trends found for CO₂, with substantial reductions in the H₂ uptakes for the wet HKUST-1 and zeolite 13x samples. Of the three more hydrophobic materials, polymer **1** has the lowest H₂ uptake

under wet conditions. Coupled with its higher CO₂ uptake, this gives **1** the highest ideal CO₂:H₂ selectivity of 22.5 (wet) and 29.9 (dry) at a pressure of 40 bar. This selectivity is four times higher than activated carbon under dry conditions, and twice as high as HKUST-1 (Table 2). Polymer **1** was also found to have the highest “wet” and “dry” ideal CO₂/H₂ selectivities at 17.5 bar, although the advantage was less pronounced because the degree of swelling is reduced at this lower pressure. However, unlike polymer **1**, the material with the next best gas selectivity at 17.5 bar, zeolite 13x, loses most of its CO₂ capacity under “wet” conditions. Thus, polymer **1** has the most promising combination of gravimetric CO₂ capacity, moisture tolerance, acid tolerance, and CO₂:H₂ selectivity for precombustion CCS of any of the materials tested. This polymer defines the upper performance bound for these five materials in terms of combining CO₂/H₂ selectivity with gravimetric CO₂ capacity, as shown in Figure 3f.

While CO₂:N₂ selectivity is a less crucial parameter than CO₂:H₂ selectivity for precombustion CCS, air ingress or incomplete air separation can lead to some nitrogen impurities in the gas stream. We therefore also calculated ideal CO₂:N₂ selectivities for each of these materials at 40 bar and at 17.5 bar (Table 2; Figure S8). As for hydrogen, the ideal wet and dry CO₂:N₂ selectivities for polymer **1** were better than for the other adsorbents, with the exception of ZIF-8, which showed similar CO₂:N₂ selectivity at 17.5 bar (Table 2).

The large CO₂ uptake for polymer **1** relative to its modest apparent BET surface area (Table 1) suggested that swelling was occurring, and that swelling was the underlying cause of both the isotherm shape (Figure 3a) and the high CO₂:H₂ selectivity for this polymer. This was confirmed by images recorded using a high-pressure view cell (S10 – S13). Polymer **1** swells by 11.2% ($\pm 1.3\%$) at 298 K and 40 bar pressure in pure CO₂, while activated carbon, and the other materials tested here, show no apparent swelling under the same conditions. At higher CO₂ pressures (60 bar), polymer **1** swells even more, by up to $55 \pm 3\%$ of the original sample volume (Figure S13). Polymer **1** also swells in CO₂ at 17.5 bar by $\sim 4.3\%$ (Figures S14 and S15). Approximately, the bulk polymer volume increases linearly as a function of CO₂ density (Figure S16). Next-generation gasifier technologies have been proposed to function at total system pressures up to 60 bar, and under those conditions, polymer **1** might perform even better than the rigid sorbents, all of which, with the exception of ZIF-8, saturate with CO₂ at a partial CO₂ pressure of 10–15 bar (Figure 3).

The swelling profile rationalizes the shape and magnitude of the CO₂ sorption isotherm in Figure 3a, and the fact that **1**, uniquely, does not reach saturation even at 40 bar. At elevated pressures, therefore, these hyper-cross-linked polymers adsorb CO₂ by a fundamentally different mechanism compared to rigid adsorbents. This explains the superior precombustion CCS properties for polymer **1**. The absence of this swelling mechanism in **1** at lower pressures also rationalizes the more modest sorption CO₂ capacities observed at 1 bar.³⁰ This swelling in CO₂ is totally and rapidly reversible over multiple pressure cycles, and hence deswelling contributes to the slope of the desorption isotherm shown in Figure 3a. The energetics (heat flow) of this swelling phenomenon might be also important in a real-life process, but this was not studied here.

Swelling enhances the working capacity of **1** with respect to nonswellable materials for pressure-swing desorption because an additional effect, deswelling, contributes to the expulsion of

CO₂ from the material during depressurization. The polymer does not swell in either H₂ or N₂ at 298 K and 40 bar (Figure S17 and S18) and hence the uptake of these gases is low, even though the low-temperature sorption isotherm for **1** (Figure 2) does suggest some swelling in liquefied N₂ at 77 K. Even allowing for the increase in sample volume with swelling, the volumetric CO₂ capacity for polymer **1** at 40 bar CO₂ (4.61 mmol/cm³; Table 2) is higher than the other adsorbents tested. The degree of swelling in pure CO₂ is proportional to the number of equivalents of cross-linker used: fewer cross-links allow more swelling (Figure S19). This could be used, potentially, to tune this behavior if more or less swelling was desired for practical application. With high equivalents of dimethyl ether, the swelling in CO₂ can be effectively shut off.

The selectivities quoted so far are ideal selectivities, calculated from separate, single-component isotherms for pure gases. In a mixed gas stream, it is conceptually possible that the additional surface area that is generated by CO₂-induced swelling could also contribute to H₂ or N₂ sorption, thus lowering the actual gas selectivity. Likewise, the polymer is likely to swell less in CO₂ that is diluted with H₂ or N₂. To test this, the swelling of **1** was measured in a gas stream comprising both CO₂ and N₂ (30:70 mol/mol) using a high-pressure view cell. This showed that the polymer also swells in a mixed gas system, but the degree of swelling was decreased as a result of the nitrogen diluent (Figure S20). The same measurement was carried out for a CO₂ and H₂ (40:60 mol/mol) mixed gas stream, which is more representative of a likely precombustion gas stream. Again, the polymer was observed to swell, but to a lesser extent than in pure CO₂ (Figure S21).

We also carried out experiments for polymer **1**, with the same mixed gas streams, using *in situ* ATR-FTIR spectroscopy⁵³ that is sensitive only to CO₂ sorption, but not to N₂ or H₂ sorption (Figure 4a; Figures S22, S23). As expected, the relative CO₂ uptake measured with 30 mol %, nitrogen-diluted CO₂, and 40 mol % hydrogen-diluted CO₂ were lower than for pure, 100 mol % CO₂. However, the reduction in CO₂ uptake was not proportional to the change in the molar gas composition. At 40 bar total pressure, the CO₂ uptake in polymer **1** for 30 mol % CO₂ was 73%, and for 40 mol % was 88%, of the CO₂ uptake measured using the same spectroscopic method for pure, 100 mol % CO₂ (Figure 4b; Figure S24). This demonstrates true chemoselectivity for polymer **1** in mixed gas streams, as required for real-life precombustion CCS.

CONCLUSIONS

A hyper-cross-linked polymer has been shown to swell in CO₂, leading to an unusual isotherm shape and high CO₂:H₂ selectivity. A number of factors remain to be explored in terms of scale up. It would be necessary to produce pellets of this polymer with sufficient mechanical robustness for use in large scale CCS. In terms of process engineering, physical swelling of the adsorbent might present challenges, although this swelling appears to be tunable to some extent (Figure S19). The detailed kinetics of swelling/deswelling should also be investigated, although preliminary view-cell studies suggest that this is both reversible and rapid (time scale of seconds). Likewise, the energetics of swelling and deswelling, and their impact on the pressure-swing process, would also need to be explored. It would certainly be preferable to devise a synthetic route that could avoid the use of large volumes of organic solvents, perhaps by synthesizing the material in a solvent-free bulk reaction, and then stripping off unreacted aromatics.

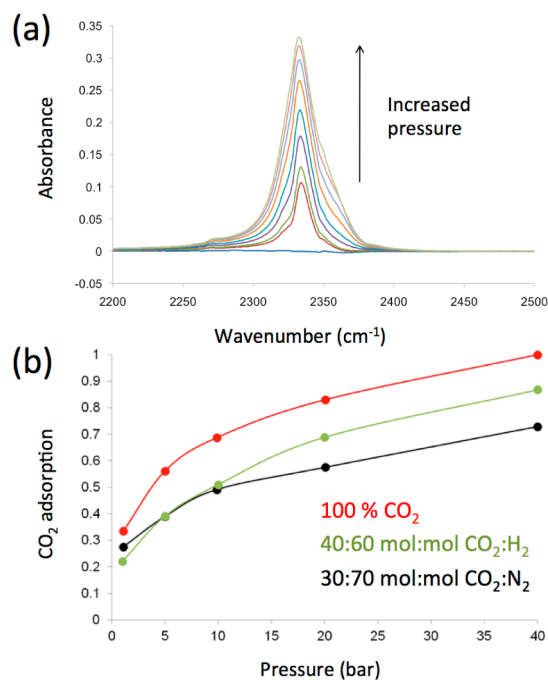


Figure 4. (a) *In situ* ATR-FTIR spectra showing the asymmetric stretching mode of physisorbed CO₂ at 2334 cm⁻¹ in polymer **1** in the 0–40 bar pressure range. This was used to calculate the CO₂ uptake in **1** as a function of increasing pressure, both for pure CO₂ and for mixed CO₂/N₂ and CO₂/H₂ systems. Neither N₂ nor H₂ have any absorbance in this region. (b) Calculated CO₂ adsorption in **1** as a function of pressure for 100 mol % CO₂ (red circles), a CO₂:H₂ mix (40:60 mol/mol) (green circles), and a CO₂:N₂ mix (30:70 mol/mol) (black circles), as measured by *in situ* ATR-FTIR. The measurements are not precisely quantitative because the refractive index of the polymers is unknown. Hence, the 30 and 40 mol % CO₂ data are normalized relative to the 100 mol % CO₂ data. The reduction in CO₂ adsorption for the diluted CO₂ mixtures is not proportional to the change in the molar gas composition, suggesting chemoselectivity toward CO₂.

Hence, as for all new porous adsorbents, there is potential for one or more of these cost or engineering factors to thwart scale up. Nonetheless, based on a range of relevant practical criteria, hyper-cross-linked polymers such as **1** appear to have strong potential as adsorbents for precombustion CCS. The polymers are robust, exceptionally tolerant to water and even to concentrated acid and, unlike many microporous polymers, polymer **1** can be prepared without using precious metal catalysts. While not tested here, this aromatic polymer should also have good stability toward corrosive impurities, such as hydrogen sulfide, which could cause problems with other porous frameworks.

Another potential advantage is cost. One of the monomers for **1**, benzene, is among the cheapest organic feedstocks possible for materials of this type, and the dimethyl acetal, while more expensive, is also a simple, commodity chemical. Analogous polymers might be produced from even cruder feedstocks, such as benzene–toluene–xylene (BTX) mixtures obtained directly from the catalytic reforming of naphtha. However, despite its synthetic simplicity, this acid-stable polymer strongly outperforms the other materials tested here in terms of both CO₂ capacity and ideal CO₂:H₂ selectivity. It also does this in the presence of adsorbed impurities, such as water vapor, which can totally undermine the CCS performance of more polar adsorbents, even if they are water-stable.

The underlying swelling mechanism is a unique feature of hyper-cross-linked polymers that has not, hitherto, been appreciated in connection with precombustion CCS. Other porous polymers have been shown recently to adsorb similar amounts of CO₂, and it is possible that swelling also occurs in these cases.^{54,55} This chemoselective swelling phenomenon might also prove useful in applications other than precombustion CO₂ capture, such as CO₂ storage or purification at moderate pressures.

■ ASSOCIATED CONTENT

Supporting Information

Details of the polymer synthesis, DNP sample preparation, characterization, further gas sorption data, IR data, and ¹³C CP MAS NMR spectra. This material is available free of charge via the Internet at <http://pubs.acs.org>.

■ AUTHOR INFORMATION

Corresponding Author

aicooper@liv.ac.uk

Notes

The authors declare no competing financial interest.

■ ACKNOWLEDGMENTS

We thank Rob Clowes for assistance with gas sorption measurements. The water isotherms were performed by Martin Smith of Dstl, Porton Down, Salisbury SP4 0JQ, Wilts, U.K. We also thank Drs Shane Pawsey, Marc A. Caporini, and Melanie Rosay (Bruker Biospin Corporation) for access to the DNP NMR spectrometer at 14.1 T. The authors would like to thank the E.ON-EPSCRC strategic call on CCS for funding (EP/G061785/1). A.I.C. is a Royal Society Wolfson Merit Award holder. T.R. thanks Mahidol University for funding.

■ REFERENCES

- (1) Haszeldine, R. S. *Science* **2009**, *325*, 1647–1652.
- (2) Schell, J.; Casas, N.; Mazzotti, M. *Energy Procedia* **2009**, *1*, 655–660.
- (3) Chiesa, P.; Consonni, S.; Kreutz, T.; Williams, R. *Int. J. Hydrogen Energy* **2005**, *30*, 747–767.
- (4) Lin, H. Q.; Freeman, B. D. *J. Mol. Struct.* **2005**, *739*, 57–74.
- (5) Carta, M.; Malpass-Evans, R.; Corad, M.; Rogan, Y.; Jansen, J. C.; Bernardo, P.; Bazzarelli, F.; McKeown, N. B. *Science* **2013**, *339*, 303–307.
- (6) Drage, T. C.; Blackman, J. M.; Pevida, C.; Snape, C. E. *Energy Fuels* **2009**, *23*, 2790–2796.
- (7) Sircar, S.; Golden, T. C.; Rao, M. B. *Carbon* **1996**, *34*, 1–12.
- (8) Casas, N.; Schell, J.; Joss, L.; Mazzotti, M. *Sep. Purif. Technol.* **2013**, *104*, 183–192.
- (9) Eddaoudi, M.; Kim, J.; Rosi, N.; Vodak, D.; Wachter, J.; O’Keefe, M.; Yaghi, O. M. *Science* **2002**, *295*, 469–472.
- (10) Côté, A. P.; Benin, A. I.; Ockwig, N. W.; O’Keefe, M.; Matzger, A. J.; Yaghi, O. M. *Science* **2005**, *310*, 1166–1170.
- (11) Millward, A. R.; Yaghi, O. M. *J. Am. Chem. Soc.* **2005**, *127*, 17998–17999.
- (12) D’Alessandro, D. M.; Smit, B.; Long, J. R. *Angew. Chem., Int. Ed.* **2010**, *49*, 6058–6082.
- (13) Keskin, S.; van Heest, T. M.; Sholl, D. S. *ChemSusChem* **2010**, *3*, 879–891.
- (14) Farha, O. K.; Eryazici, I.; Jeong, N. C.; Hauser, B. G.; Wilmer, C. E.; Sarjeant, A. A.; Snurr, R. Q.; Nguyen, S. T.; Yazaydin, A. O.; Hupp, J. T. *J. Am. Chem. Soc.* **2012**, *134*, 15016–15021.
- (15) Furukawa, H.; Ko, N.; Go, Y. B.; Aratani, N.; Choi, S. B.; Choi, E.; Yazaydin, A. O.; Snurr, R. Q.; O’Keefe, M.; Kim, J.; Yaghi, O. M. *Science* **2010**, *329*, 424–428.
- (16) Deng, H.; Doonan, C. J.; Furukawa, H.; Ferreira, R. B.; Towne, J.; Knobler, C. B.; Wang, B.; Yaghi, O. M. *Science* **2010**, *327*, 846–850.
- (17) Banerjee, R.; Phan, A.; Wang, B.; Knobler, C.; Furukawa, H.; O’Keefe, M.; Yaghi, O. M. *Science* **2008**, *319*, 939–943.
- (18) Liu, X.; Li, Y.; Ban, Y.; Peng, Y.; Jin, H.; Xu, L.; Caro, J.; Yang, W. *Chem. Commun.* **2013**, *49*, 9140–9142.
- (19) McKeown, N. B.; Budd, P. M. *Macromolecules* **2010**, *43*, 5163–5176.
- (20) Ben, T.; Ren, H.; Ma, S.; Cao, D.; Lan, J.; Jing, X.; Wang, W.; Xu, J.; Deng, F.; Simmons, J. M.; Qiu, S.; Zhu, G. *Angew. Chem., Int. Ed.* **2009**, *48*, 9457–9460.
- (21) Xu, Y.; Jin, S.; Xu, H.; Nagai, A.; Jiang, D. *Chem. Soc. Rev.* **2013**, *42*, 8012–8031.
- (22) Dawson, R.; Cooper, A. I.; Adams, D. J. *Polym. Int.* **2013**, *62*, 345–352.
- (23) Dawson, R.; Adams, D. J.; Cooper, A. I. *Chem. Sci.* **2011**, *2*, 1173–1177.
- (24) Rabbani, M. G.; El-Kaderi, H. M. *Chem. Mater.* **2011**, *23*, 1650–1653.
- (25) Lu, W. G.; Yuan, D.; Sculley, J.; Zhao, D.; Krishna, R.; Zhou, H.-C. *J. Am. Chem. Soc.* **2011**, *133*, 18126–18129.
- (26) Kazarian, S. G.; Vincent, M. F.; Bright, F. V.; Liotta, C. L.; Eckert, C. A. *J. Am. Chem. Soc.* **1996**, *118*, 1729–1736.
- (27) Dawson, R.; Stevens, L.; Drage, T.; Snape, C. E.; Smith, M. W.; Adams, D. J.; Cooper, A. I. *J. Am. Chem. Soc.* **2012**, *134*, 10741–10744.
- (28) Davankov, V. A.; Tsyurupa, M. P. *React. Polym.* **1990**, *13*, 27–42.
- (29) Tsyurupa, M. P.; Davankov, V. A. *React. Funct. Polym.* **2006**, *66*, 768–779.
- (30) Li, B. Y.; Gong, R.; Wang, W.; Huang, H.; Zhang, W.; Li, H.; Hu, C.; Tan, B. *Macromolecules* **2011**, *44*, 2410–2414.
- (31) Martin, C. F.; Stöckel, E.; Clowes, R.; Adams, D. J.; Cooper, A. I.; Pis, J. J.; Rubiera, F.; Pevida, C. *J. Mater. Chem.* **2011**, *21*, 5475–5483.
- (32) Tsyurupa, M. P.; Papkov, M. A.; Davankov, V. A. *Polym. Sci., Ser. C* **2009**, *51*, 81–86.
- (33) Davankov, V. A.; Pastukhov, A. V. *J. Phys. Chem. B* **2011**, *115*, 15188–15195.
- (34) Hilic, S.; Boyer, S. A. E.; Padua, A. A. H.; Grolier, J. P. E. *J. Polym. Sci., Part B: Polym. Phys.* **2001**, *39*, 2063–2070.
- (35) Hall, D. A.; Maus, D. C.; Gerfen, G. J.; Inati, S. J.; Becerra, L. R.; Dahlquist, F. W.; Griffin, R. G. *Science* **1997**, *276*, 930–932.
- (36) Rosay, M.; Tometich, L.; Pawsey, S.; Bader, R.; Schauwecker, R.; Blank, M.; Borchard, P. M.; Cauffman, S. R.; Felch, K. L.; Weber, R. T.; Griffin, R. G.; Maas, W. E. *Phys. Chem. Chem. Phys.* **2010**, *12*, 5850–5860.
- (37) Lesage, A.; Lelli, M.; Gajan, D.; Caporini, M. A.; Vitzthum, V.; Miéville, P.; Alauzan, J.; Roussey, A.; Thieuleux, C.; Mehdi, A.; Bodenhausen, G.; Copéret, C.; Emsley, L. *J. Am. Chem. Soc.* **2010**, *132*, 15459–15461.
- (38) Takahashi, H.; Lee, D.; Dubois, L.; Bardet, M.; Hediger, S.; De Paëpe, G. *Angew. Chem., Int. Ed.* **2012**, *51*, 11766–11769.
- (39) Zhe Ni, Q.; Daviso, E.; Can, T. V.; Markhasin, E.; Jawla, S. K.; Swager, T. M.; Temkin, R. J.; Herzfeld, J.; Griffin, R. G. *Acc. Chem. Res.* **2013**, *46*, 1933–1941.
- (40) Rossini, A. J.; Zagdoun, A.; Lelli, M.; Lesage, A.; Copéret, C.; Emsley, L. *Acc. Chem. Res.* **2013**, *46*, 1942–1951.
- (41) Ouari, O.; Phan, T.; Ziarelli, F.; Casano, G.; Aussenac, F.; Thureau, P.; Gigmès, D.; Tordo, P.; Viel, S. *ACS Macro Lett.* **2013**, *2*, 715–719.
- (42) Song, C.; Hu, K.-N.; Joo, C.-G.; Swager, T. M.; Griffin, R. G. *J. Am. Chem. Soc.* **2006**, *128*, 11385–11390.
- (43) Matsuki, Y.; Maly, T.; Ouari, O.; Karoui, H.; Le Moigne, F.; Rizzatto, E.; Lyubenova, S.; Herzfeld, J.; Prisner, T.; Tordo, P.; Griffin, R. G. *Angew. Chem., Int. Ed.* **2009**, *48*, 4996–5000.
- (44) Zagdoun, A.; Casano, G.; Ouari, O.; Schwarzwälder, M.; Rossini, A. J.; Aussenac, F.; Yulikov, M.; Jeschke, G.; Copéret, C.; Lesage, A.; Tordo, P.; Emsley, L. *J. Am. Chem. Soc.* **2013**, *135*, 12790–12797.

- (45) Blanc, F.; Chong, S. Y.; McDonald, T. O.; Adams, D. J.; Pawsey, S.; Caporini, M. A.; Cooper, A. I. *J. Am. Chem. Soc.* **2013**, *135*, 15290–15293.
- (46) Jeromenok, J.; Weber, J. *Langmuir* **2013**, *29*, 12982–12989.
- (47) Ko, D.; Siriwardane, R.; Biegler, L. T. *Ind. Eng. Chem. Res.* **2003**, *42*, 339–348.
- (48) Chui, S. S. Y.; Lo, S. M. F.; Charmant, J. P. H.; Orpen, A. G.; Williams, I. D. *Science* **1999**, *283*, 1148–1150.
- (49) Liang, Z.; Marshall, M.; Chaffee, A. L. *Energy Fuels* **2009**, *23*, 2785–2789.
- (50) Yazaydin, A. O.; Benin, A. I.; Faheem, S. A.; Jakubczak, P.; Low, J. J.; Willis, R. R.; Snurr, R. Q. *Chem. Mater.* **2009**, *21*, 1425–1430.
- (51) Kizzie, A. C.; Wong-Foy, A. G.; Matzger, A. J. *Langmuir* **2011**, *27*, 6368–6373.
- (52) Bhatia, S. K.; Myers, A. L. *Langmuir* **2006**, *22*, 1688–1700.
- (53) Hasell, T.; Armstrong, J. A.; Jelfs, K. E.; Tay, F. H.; Thomas, M.; Kazarian, S. G.; Cooper, A. I. *Chem. Commun.* **2013**, *49*, 9410–9412.
- (54) Patel, H. A.; Karadas, F.; Canlier, A.; Park, J.; Deniz, E.; Jung, Y.; Atilhan, M.; Yavuz, C. T. *J. Mater. Chem.* **2012**, *22*, 8431–8437.
- (55) Patel, H. A.; Karadas, F.; Byun, J.; Park, J.; Deniz, E.; Canlier, A.; Jung, Y.; Atilhan, M.; Yavuz, C. T. *Adv. Funct. Mater.* **2013**, *23*, 2270–2276.